ENCLOSURE A

DB-1 CRDM NOZZLE WELD ANOMALY FLAW EVALUATION OF IDTB REPAIR

(NONPROPRIETARY VERSION)

AREVA CALCULATION 32-9134666-002

Forty-Two Pages Follow

AREVA

CALCULATION SUMMARY SHEET (CSS)

Document No. 32 - 9135800 - 000 Safety Related: ☒ Yes ☐ No

Title DB-1 CRDM Nozzle Weld Anomaly Flaw Evaluation of IDTB Repair

PURPOSE AND SUMMARY OF RESULTS:

This document is a non-proprietary version of AREVA NP Document number 32-9134666-002. The proprietary information removed from 32-9134666-002 is indicated by a pair of square brackets "[ ]". The geometry and operating conditions are FirstEnergy Corporation Proprietary and other relevant information are AREVA NP, Inc. Proprietary.

The purpose of this analysis is to perform a fracture mechanics evaluation of a postulated anomaly in the Davis-Besse Unit 1 (DB-1) Control Rod Drive Mechanism (CRDM) nozzle ID temper bead weld. This anomaly is assumed to be a 0.1 inch semi-circular flaw extending 360 degrees around the circumference at the "triple point" location where there is a confluence of three materials; the Alloy 600 nozzle, the Alloy 52M weld, and low alloy steel head. Two potential flaw propagation paths are considered in the flaw evaluations. The analysis includes prediction of fatigue crack growth in an air environment since the anomaly is located on the outside surface of the new weld, just below the bottom of the severed nozzle. Flaw acceptance is based on the 1995 through 1996 ASME Code Section XI criteria for applied stress intensity factor (IWB-3612) and limit load (IWB-3642).

The results of the analysis demonstrate that the 0.1 inch weld anomaly is acceptable for a 25 year evaluation life of the CRDM nozzle ID temper bead weld repair. However, note that the design life of the RVCH, as per the design specification is 4 years (Ref. 2). Significant fracture toughness margins have been demonstrated for each of the two flaw propagation paths considered in the analysis. The minimum fracture toughness margin is 3.88, compared to the required margins of $\sqrt{10}$ for normal/upset conditions and $\sqrt{2}$ for emergency/faulted conditions per IWB-3612. Fatigue crack growth is minimal since the maximum final flaw size is [ ] inch. The margin on limit load is 10.44 for normal/upset conditions and 7.38 for emergency/faulted conditions, compared to the required margins of 3.0 and 1.5, respectively, per IWB-3642.

THE FOLLOWING COMPUTER CODES HAVE BEEN USED IN THIS DOCUMENT:

CODE/VERSION/REV	CODE/VERSION/REV

THE DOCUMENT CONTAINS ASSUMPTIONS THAT SHALL BE VERIFIED PRIOR TO USE

☐ YES
☒ NO

Controlled Document

AREVA
AREVA NP Inc.,
an AREVA and Siemens company

0402-01-F01 (20697) (Rev. 014, 04/13/2009)

Document No. 32-9135800-000

DB-1 CRDM Nozzle Weld Anomaly Flaw Evaluation of IDTB Repair

Review Method: ☒ Design Review (Detailed Check)
☐ Alternate Calculation

Signature Block

Name and Title (printed or typed)	Signature	P/R/A and LP/LR	Date	Pages/Sections Prepared/Reviewed/Approved
S. J. Noronha Engineer IV	SJNoronha	P	04/08/10	All
Heqin Xu Engineer IV		LR	4/8/10	All (Detailed check)
Miao Sun Engineer III		R	4/8/2010	Appendix A
T. M. Wiger Manager	T.M. Wiger	A	4/8/10	All

Note: P/R/A designates Preparer (P), Reviewer (R), Approver (A);
LP/LR designates Lead Preparer (LP), Lead Reviewer (LR)

Project Manager Approval of Customer References (N/A if not applicable)

Name (printed or typed)	Title (printed or typed)	Signature	Date
N/A			

Mentoring Information (not required per 0402-01)

Name (printed or typed)	Title (printed or typed)	Mentor to: (P/R)	Signature	Date
N/A				

DB-1 CRDM Nozzle Weld Anomaly Flaw Evaluation of IDTB Repair

Record of Revision

Revision No.	Date	Pages/Sections/ Paragraphs Changed	Brief Description / Change Authorization
000	04/2010	ALL	Original

Table of Contents

Table of Contents
(continued)

List of Tables

List of Figures

1.0 INTRODUCTION

The purpose of this analysis is to perform a fracture mechanics evaluation of a postulated anomaly in the Davis-Besse Unit 1 (DB-1) Control Rod Drive Mechanism (CRDM) nozzle ID temper bead weld. This anomaly is assumed to be a 0.1 inch semi-circular flaw extending 360 degrees around the circumference at the "triple point" location where there is a confluence of three materials; the Alloy 600 nozzle, the Alloy 52M weld, and low alloy steel head. Two potential flaw propagation paths are considered in the flaw evaluations.

1.1 CRDM Nozzle IDTB Weld Repair

The CRDM nozzle ID temper bead (IDTB) weld repair is described by the design drawing (Ref.1). This weld repair establishes a new pressure boundary above the original J-groove weld. The five steps involved in the repair design are listed below.

1) Roll Expansion
2) Nozzle Removal and Weld Prep Machining
3) Welding
4) Grinding/Machining and NDE
5) Original Weld Grinding

During the welding process (step 3), a maximum 0.1 inch weld anomaly may be formed due to lack of fusion at the "triple point", as shown in Figure 1-1. The anomaly is conservatively assumed to be a "crack-like" defect 360° around the circumference at the "triple point" location. The technical requirements document (Ref.2) provides additional details of the ID temper bead weld repair procedure. The purpose of the present fracture mechanics analysis is to provide justification, in accordance with Section XI of the ASME Code (Ref.3), for operating with the postulated weld anomaly at the triple point. Predictions of fatigue crack growth are based on an evaluation life of 25 years.

1.2 Potential Weld Anomaly

The anomaly could be located in the triple point region as shown in Figure 1-1. The region is called a "triple point" since three materials intersect at this location. The materials are:

a) the Alloy 600 CRDM nozzle material,
b) the new ERNiCrFe-7A filler weld material,* and
c) the low alloy steel RV head material.

* Per Ref. 4, Specification 5.14, Par. A7.4.3, "Filler metal of this classification is used for welding nickel-chromium-iron alloy (ASTM B163, B166, B167, and B168 having UNS Number N06690)." This UNS number is associated with Alloy 690 material.

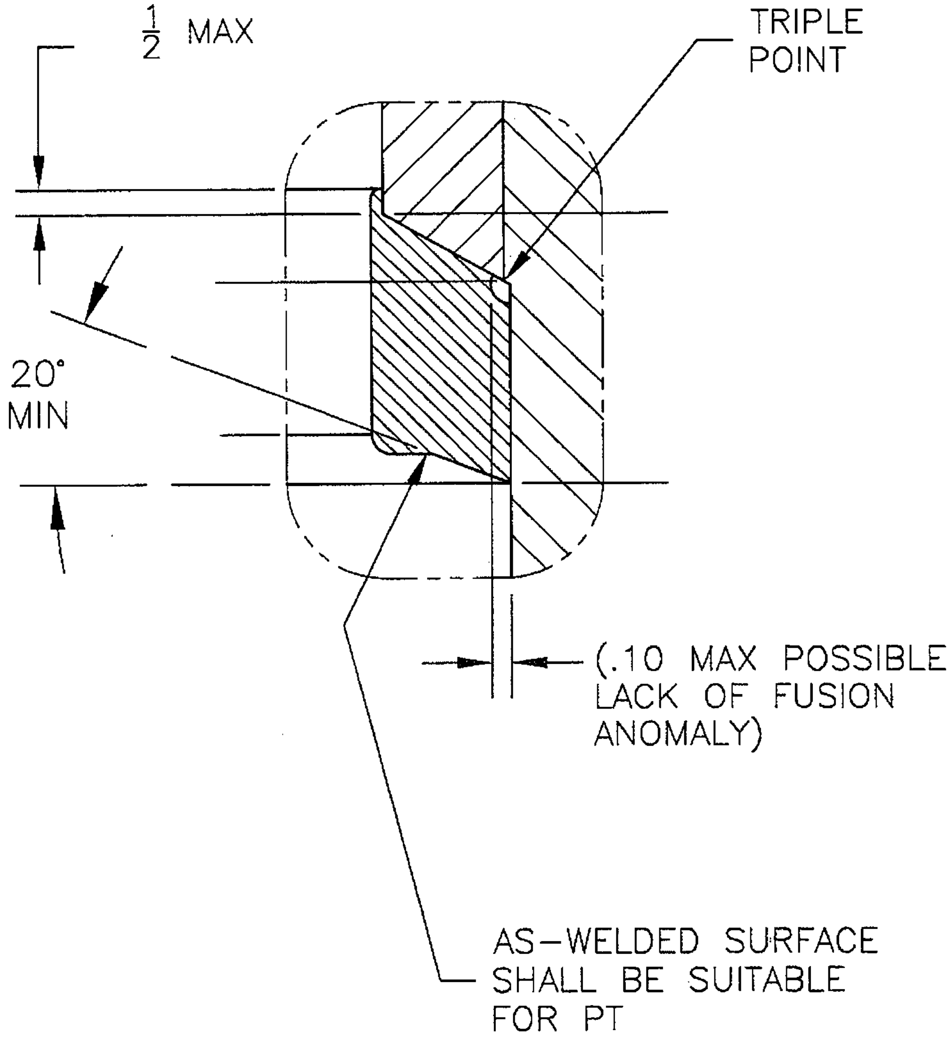

Figure 1-1: Weld Anomaly in Temper Bead Weld Repair

1.3 Postulated Flaws

The triple point weld anomaly is assumed to be semi-circular in shape with an initial radius of 0.10", as indicated in Figure 1-1. It is further assumed that the anomaly extends 360° around the nozzle. Three flaws are postulated to simulate various orientations and propagation directions for the anomaly. A circumferential flaw and an axial flaw on the outside surface of the nozzle would both propagate in a horizontal direction toward the inside surface. A cylindrically oriented flaw along the interface between the weld and head would propagate downward between the two components. The horizontal and vertical flaw propagation directions are represented in Figure 1-2 by separate paths for the downhill and uphill sides of the nozzle, as discussed below. For both these directions, fatigue crack growth will be calculated considering the most susceptible material for flaw propagation.

Horizontal Direction (Path 1):

> Flaw propagation is across the CRDM tube wall thickness from the OD of the tube to the ID of the tube. This is the shortest path through the component wall, passing through the new Alloy 690 weld material. However, Alloy 600 tube material properties or equivalent are used for axial flaw evaluations to ensure that another potential path through the HAZ between the new repair weld and the Alloy 600 tube material is bounded.
>
> For completeness, two types of flaws are postulated at the outside surface of the tube. A 360° continuous circumferential flaw, lying in a horizontal plane, is considered to be a conservative representation of crack-like defects that may exist in the weld anomaly. This flaw would be subjected to axial stresses in the tube. An axially oriented semi-circular outside surface flaw is also considered since it would lie in a plane that is normal to the higher circumferential stresses. Both of these flaws would propagate toward the inside surface of the tube.

Vertical Direction (Path 2):

> Flaw propagation is down the outside surface of the repair weld between the weld and RV head. A continuous surface flaw is postulated to lie along this cylindrical interface between the two materials. This flaw, driven by radial stresses, may propagate along either the new Alloy 690 weld material or the low alloy steel head material.

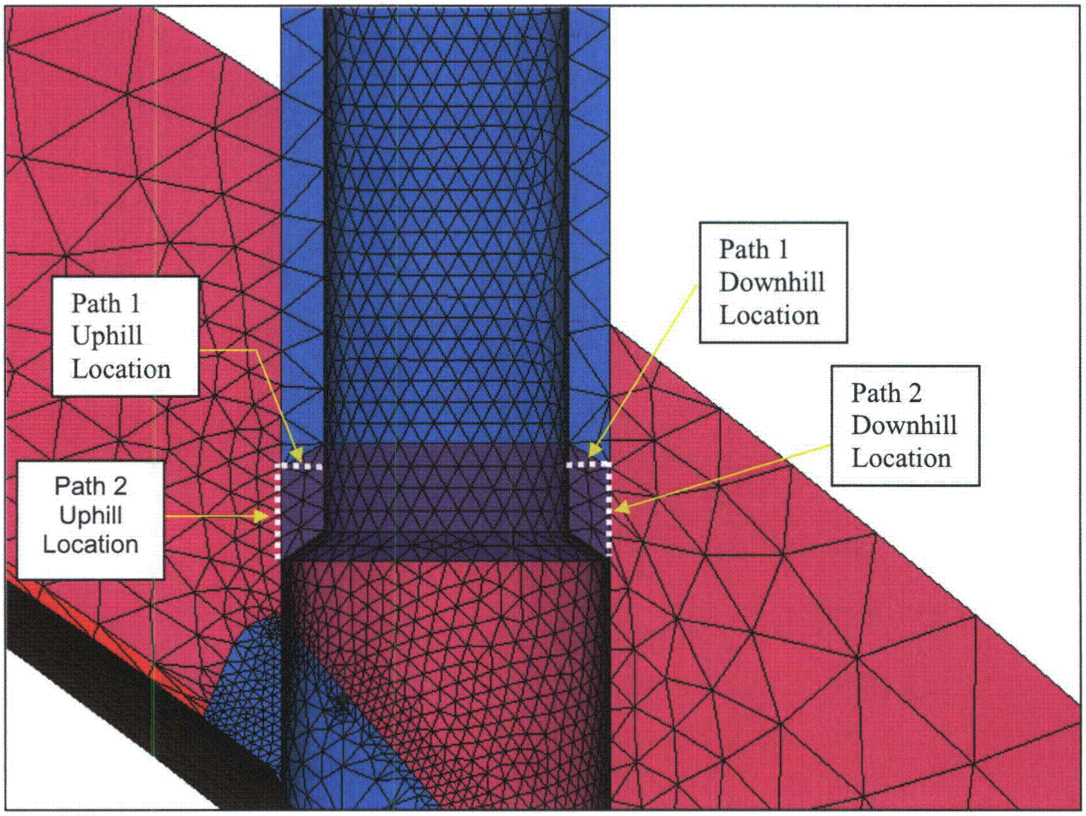

Figure 1-2: Illustration of Crack Propagation Paths on the Finite Element Stress Model

2.0 ANALYTICAL METHODOLOGY

This section presents several aspects of linear elastic fracture mechanics (LEFM) and limit load analysis (to address the ductile Alloy 600 and Alloy 690 materials) that form the basis of the present flaw evaluations. As discussed in Section 1.3, flaw evaluations are performed for flaw propagation Paths 1 and 2 in Figure 1-2.

2.1 SIF Solutions

Path 1 represents a section across the new Alloy 52M weld metal which is equivalent to the thickness of the CRDM tube wall. Since the weld anomaly is located at the base of the OD of the CRDM tube and is assumed to be all the way around the circumference, a stress intensity factor (SIF) solution for a 360° circumferential crack on the OD of a circular tube is deemed appropriate. Therefore, the SIF solution of Buchalet and Bamford (Ref.5) is used in the analysis. However, this solution is applicable to a 360° part-through ID flaw. To develop an SIF solution for a 360° part-through OD flaw, an F function is determined based on SIF solutions of Kumar (Ref.6 and Ref.7). Appropriate F functions for internal and external circumferential flaws are determined for a cylinder subjected to remote tension. The ratio of the F functions for the external and internal flaws is considered to be an appropriate multiplying factor for the Buchalet and Bamford SIF solution to extend its application to an external flaw. Similar ratios have been reported by Kumar (Ref.8). The materials to be considered for this path are the Alloy 600 tube material or the Alloy 52M weld metal. Fatigue crack growth is calculated using crack growth rates for austenitic stainless steels from Appendix C of Section XI (Ref.3). A limit load analysis for an external circumferential flaw in a cylinder subjected to remote tension (Ref.7) is also performed for applied loads on the CRDM tube.

An axially oriented semi-circular OD surface flaw is also considered in the evaluation, as illustrated by the schematic below.

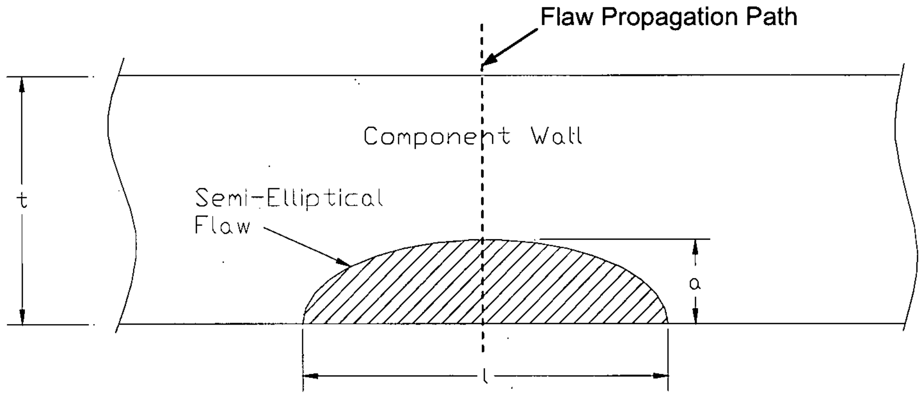

where,
a = initial flaw depth = 0.100 inch
l = 2c = flaw length = 0.200 inch
t = wall thickness = [ ] inch

An axial flaw is considered since the stresses in the CRDM penetration region are primarily due to pressure and therefore the hoop stresses are more significant. The SIF solution by Raju & Newman (Ref.9) for an external surface crack in a cylindrical vessel is used in the evaluation, considering growth in both the radial and axial directions. The fatigue flaw growth analysis for the axial crack is also performed using the austenitic stainless steel crack growth rates.

The Irwin plasticity correction is also considered in the SIF solutions discussed above. This plastic zone correction is discussed in detail in Section 2.8.1 of (Ref.10). The effective crack length is defined as the sum of the actual crack size and the plastic zone correction:

$$a_e = a + r_y$$

where r_y for plane strain conditions (applicable for this analysis) is given by:

$$r_y = \frac{1}{6\pi}\left(\frac{K_I}{\sigma_{YS}}\right)^2$$

Path 2 represents the interface between the new repair weld and the RV head material. The potential for flaw propagation along this interface is likely if radial stresses are significant between the weld and head. This assessment utilizes an SIF solution for a continuous surface crack in a flat plate from Appendix A of the 1995 Edition of Section XI (Ref.3). Flat plate solutions are routinely used to evaluate flaws in cylindrical components such as the repair weld since the added constraint provided by the cylindrical structure reduces the crack opening displacements. The solution is therefore inherently conservative for this application. Crack growth analysis is performed considering propagation through the Alloy 52M weld metal or the low alloy steel head material, whichever is limiting.

2.2 Fatigue Crack Growth

Flaw growth due to fatigue is characterized by

$$\frac{da}{dN} = C_o(\Delta K_I)^n$$

where C_o and n are constants that depend on the material and environmental conditions, ΔK_I is the range of applied stress intensity factor in terms of ksi√in, and da/dN is the incremental flaw growth in terms of inches/cycle. For the embedded weld anomaly considered in the present analysis, it is appropriate to use crack growth rates for an air environment. Fatigue crack growth is also dependent on the ratio of the minimum to the maximum stress intensity factor; i.e.,

$$R = (K_1)_{min} / (K_1)_{max}$$

<u>SA-533 Grade B Class 1 Low Alloy Steel Plate Material (RV Head)</u>

From Article A-4300 of the 1995 Edition with 1996 Addendum of Section XI (Ref.3), the fatigue crack growth constants for subsurface flaws in an air environment are:

$n = 3.07$
$C_o = 1.99 \times 10^{-10}\ S$
where $S = 25.72\,(2.88 - R)^{-3.07}$ for $0 \leq R < 1$

<u>Alloy 600 and Alloy 690 Materials (used for Alloy 52M Weld Metal)</u>

Fatigue crack growth rates for austenitic stainless steels are used to conservatively predict flaw growth in the new Alloy 52M repair weld. From Article C-3210 of the 1995 Edition with 1996 Addendum of Section XI (Ref.3), the fatigue crack growth constants for subsurface flaws in an air environment are:

$n = 3.3$
$C_o = C \times S$
where $C = 10^{[-10.009 + 8.12E\text{-}4 \times T - 1.13E\text{-}6 \times T^2 + 1.02E\text{-}9 \times T^3]}$
$S = 1.0$ for $R \leq 0$
$= 1.0 + 1.8R$ for $0 < R \leq 0.79$
$= -43.35 + 57.97R$ for $0.79 < R < 1.0$

2.3 Acceptance Criteria

The low alloy steel reactor vessel head material will be evaluated against the IWB-3612 acceptance criteria of Section XI (Ref. 3). For the highly ductile materials Alloy 600 and Alloy 690 materials, the initial flaw depth to thickness ratio for the postulated weld anomaly is only about 20% and fatigue crack growth is minimal for these materials in an air environment. A convenient acceptance criterion on flaw size is the industry developed 75% through-wall limit on depth (Ref. 11):

$$\frac{a}{t} \leq 0.75$$

For the shallow cracks considered in the present analysis, this criterion is easily met. In addition, stress intensity factors will be calculated and evaluated against conservative fracture toughness requirements using a factor of safety of √10 for normal and upset conditions.

Another acceptance criterion for ductile materials is demonstration of sufficient limit load margin. From IWB-3642 (Ref. 3), the required safety margin, based on load, is a factor of 3 for normal and upset conditions and a factor of 1.5 for emergency and faulted conditions.

Since stresses for emergency/faulted conditions are bounded by the controlling normal/upset condition stresses (see Section 4.2) and the required fracture toughness margins are less stringent for emergency/faulted conditions, satisfying normal/upset conditions requirements implicitly satisfies those for emergency/faulted conditions as well.

3.0 ASSUMPTIONS

This analysis contains no major assumptions that must be verified prior to use on safety-related work. Listed below are minor assumptions that are pertinent to the present fracture mechanics evaluation.

1) The anomaly is assumed to include a "crack-like" defect, located at the triple-point location and extending all the way around the circumference. For analytical purposes, a continuous circumferential flaw is located in the horizontal plane at the top of the weld. Another continuous flaw is located in the cylindrical plane between the weld and reactor vessel (RV) head.
2) In the radial plane, the anomaly is assumed to include a quarter-circular "crack-like" defect (see Figure 1-1). For analytical purposes, a semi-circular flaw is used to represent the radial cross-section of the anomaly.
3) An RT_{NDT} value of 60°F is conservatively assumed for the SA-533 Grade B Class 1 low alloy reactor vessel head material. This is based on a highest measured value of 40°F for 13 heats of SA-533 Grade B plate material (Ref.12).

4.0 DESIGN INPUTS

The region of interest for the present flaw evaluations is at the triple point, where three different materials intersect. These materials are the CRDM nozzle material, the new weld material and the reactor vessel head material.

The DB Unit 1 CRDM nozzles are made from Alloy 600 material to ASME specification SB-167 for tubular products (Ref. 2). The new weld, as noted in Section 1.2, is made from Alloy 690 type material. The portion of the reactor vessel head that contains the CRDM nozzles is fabricated from SA-533 Grade B Class 1 (Ref. 2). The normal operating temperature as per the input information from FirstEnergy is [ ] °F (See Appendix B) (Ref.13).

4.1 Code Minimum Yield Strength

The code minimum yield strength, Sy, values for SB-167 Material N06600 (Alloy 600 Material) as per the 1989 edition of the ASME Code (Ref.18) is 35.0 ksi at room temperature and 27.8 ksi at operating temperature of [ ] °F.

For the SA-533 Grade B Class 1 Low Alloy Steel Material (RV Head), the room temperature yield strength is 50.0 ksi and at operating temperature ([ ] °F) the yield strength is 43.8 ksi (Ref.18).

For the Alloy 52M new weld material, the material properties are obtained from Code Case N-474-2 as per (Ref.2). The yield strength for Alloy 52M material at operating temperature of [ ] °F is 27.6 ksi.

The code minimum yield strength is used for limit load analysis. The yield strength values used for plastic zone correction of the stress intensity factor as discussed in section 5.0 are the same as the ones used for residual stress calculation.

4.2 Applied Stresses

The applied stresses are the cyclic stresses that contribute to fatigue crack growth. Incremental crack growth is based on six design heatup/cooldown cycles per year of operation. Residual stresses are also developed in the repair weld from the ID temper bead welding process that forms the new pressure boundary.

4.2.1 Fatigue Stresses

Fatigue stresses are obtained from the generic stress analysis for the B&W 177 FA plants contained in Reference14. The maximum stresses, which occur during cooldown (at 10.004 hours into the composite heatup/cooldown transient), are combined with a zero stress at shutdown to produce a maximum cyclic load since stresses remain positive during this transient due to the dominating effect of pressure. The reactor coolant pressure at the 10.004 hour time point is [ ] psig (Ref. 14). A slightly higher pressure ([ ] psia) occurs during a rod withdrawal accident, which is classified as an upset condition in the reactor coolant system functional specification (Ref.15). Stresses for the rod withdrawal transient will be obtained by multiplying the stresses at 10.004 hours into the composite heatup/cooldown transient by the ratio of the pressures for the two transients.

Component stresses are obtained for the two crack propagation paths outlined on the finite element model in (Ref. 14). Stresses for Paths 1 and 2 are obtained from (Ref.14). Stresses are reported in a cylindrical coordinate system relative to the CRDM nozzle and include the three component stresses (axial, hoop and radial) needed to calculate mode I stress intensity factors for the various postulated flaws. These stresses, provided at four uniform increments along each path, were derived for ligament thicknesses of 0.488" for Path 1 and 1.143 inches for Path 2.

The stresses in Reference 14 apply directly to a weld thickness of 0.488". After grinding the inside surface of the weld, the thickness of the weld relative to the outside surface of the nozzle is [ ] (Ref. 1). The length of the actual weld is 1.35 inches (Ref. 1). Since the actual weld thickness and length are greater than the analyzed thickness, no adjustment will be made to the Reference 14 stresses in the present flaw evaluations.

To ensure that the bounding stresses are captured for use in the present flaw evaluations, stresses are obtained at every 45 degrees from the downhill (0°) to the uphill (180°) locations, as shown by the figure in Appendix D of Reference 14. It is concluded in that reference that the most limiting path is at the 180° uphill location. The uphill stresses are presented in Tables 4-1 and 4-2 for Paths 1 and 2, respectively.

As noted in the conclusions of Appendix F of Reference 14, stresses due to emergency/faulted conditions are bounded by the controlling normal/upset condition stresses. Therefore, the emergency/faulted condition stresses are bounded by the normal/upset condition stresses, considered above, for the fatigue crack growth analysis.

Table 4-1: Stresses for Flaw Evaluations along Path 1 (Ref. 14)

Composite Heatup/Cooldown Transient (Normal Operating Conditions)

Path: **WA180** Length = 0.488 **Triple Point**

	Location:	0.000	0.000	0.000	0.122	0.122	0.122	0.244	0.244	0.244	0.366	0.366	0.366	0.488	0.488	0.488
Pressure	Time	--SX--	--SY--	--SZ--	--SX--	--SY--	--SZ--	--SX--	--SY--	--SZ--	--SX--	--SY--	--SZ--	--SX--	--SY--	--SZ--
(psig)	(hr.)	Radial	Hoop	Axial	Radial	Hoop	Axial	Radial	Hoop	Axial	Radial	Hoop	Axial	Radial	Hoop	Axial
	0.001	[														
	4.770															
	4.871															
	7.000															
	7.313															
	7.412															
	10.000															
[ ]	10.004															
	10.013															
	10.117															
	10.217															
	10.250															
	10.718															
	12.939															]

Ratioed Stresses for Rod Withdrawl Accident (Upset Condition)

Note: Rod Withdrawal Accident Stress = [ ] * Heatup/Cooldown Stress **Triple Point**

	Location:	0.000	0.000	0.000	0.122	0.122	0.122	0.244	0.244	0.244	0.366	0.366	0.366	0.488	0.488	0.488
Pressure		--SX--	--SY--	--SZ--	--SX--	--SY--	--SZ--	--SX--	--SY--	--SZ--	--SX--	--SY--	--SZ--	--SX--	--SY--	--SZ--
(psig)		Radial	Hoop	Axial	Radial	Hoop	Axial	Radial	Hoop	Axial	Radial	Hoop	Axial	Radial	Hoop	Axial
[ ]		[														]

Legend:
SX = radial stress
SY = hoop stress
SZ = axial stress

Table 4-2: Stresses for Flaw Evaluations along Path 2 (Ref. 14)

Composite Heatup/Cooldown Transient (Normal Operating Conditions)

Path: **WV180** Length = 1.143

Triple Point

Pressure (psig)	Location: Time (hr.)	0.0000 --SX-- Radial	0.0000 --SY-- Hoop	0.0000 --SZ-- Axial	0.2858 --SX-- Radial	0.2858 --SY-- Hoop	0.2858 --SZ-- Axial	0.5715 --SX-- Radial	0.5715 --SY-- Hoop	0.5715 --SZ-- Axial	0.8573 --SX-- Radial	0.8573 --SY-- Hoop	0.8573 --SZ-- Axial	1.1430 --SX-- Radial	1.1430 --SY-- Hoop	1.1430 --SZ-- Axial
	0.001	[														
	4.770															
	4.871															
	7.000															
	7.313															
	7.412															
	10.000															
[ ]	10.004															
	10.013															
	10.117															
	10.217															
	10.250															
	10.718															
	12.939															]

Ratioed Stresses for Rod Withdrawl Accident (Upset Condition)

Note: Rod Withdrawal Accident Stress = [ ]* Heatup/Cooldown Stress

Triple Point

Pressure (psig)	Location:	0.000 --SX-- Radial	0.000 --SY-- Hoop	0.000 --SZ-- Axial	0.122 --SX-- Radial	0.122 --SY-- Hoop	0.122 --SZ-- Axial	0.244 --SX-- Radial	0.244 --SY-- Hoop	0.244 --SZ-- Axial	0.366 --SX-- Radial	0.366 --SY-- Hoop	0.366 --SZ-- Axial	0.488 --SX-- Radial	0.488 --SY-- Hoop	0.488 --SZ-- Axial
[ ]		[														]

Legend:
SX = radial stress
SY = hoop stress
SZ = axial stress

4.2.2 Residual Stresses

A three-dimensional elastic-plastic finite element analysis (see (Ref. 16)) was performed to simulate the sequence of steps involved in arriving at the configuration of the CRDM nozzle and reactor vessel head after completion of the ID temper bead repair. A comparison of the geometry and materials of reactor vessel closure heads of ANO-1 and DB-1 is presented in Appendix A of this document to justify the use of the weld residual stresses from the analysis of Reference 16. To simplify the analysis of the complete repair process, only the center nozzle was modeled (Figure 4-1). Although this axisymmetric analysis was based on the geometry of the center nozzle penetration, adjustments were made to represent significant aspects of the controlling nozzle at the outermost hillside location ([ ]° from the top of the vessel). In particular, the repair weld was positioned at the minimum distance above the J-groove and the J-groove weld was chamfered to simulate the largest chamfer (7/8"). The model also used the highest yield strength of any nozzle in the head ([ ]). The [ ]° nozzle location was limiting for all three of these conditions.

The FE analysis simulated the laying of the original weld butter and the subsequent post-weld stress relief, the heatup of the original J-groove weld and adjacent material during the welding process and the subsequent cooldown to ambient temperature, a pre-service hydro test, and operation at steady state conditions. After the steady state loads were removed and the structure was again at ambient conditions, the portion of the nozzle below the cut line (Ref. 1) was deleted. Deposition of the repair weld was simulated using four weld passes, and the J-groove weld was chamfered as shown in Figure 4-2. The analysis of this final configuration provided residual stresses in the repair weld for use in the present flaw evaluations. These stresses are listed in Table 4-3 & Table 4-4.

The repair weld analysis in Ref. 16 used a multi-linear isotropic hardening model to characterize the nozzle material and elastic-perfectly plastic material models for the welds, butter, cladding and head. The yield strengths for the non-strain hardening models were selected to represent the flow stress of the various materials. The following yield strength values were used in the repair weld FE analysis:

Component	**Material**	**Yield Strength at 600 °F**
Nozzle	Alloy 600	[ ] ksi
Repair weld	Alloy 52M	[ ] ksi
J-groove weld	Alloy 182	[ ] ksi
Butter	Alloy 182	[ ] ksi
Head	Low alloy steel	[ ] ksi
Cladding	Stainless steel	[ ] ksi

*Note, the operating temperature of the plant is [ ] °F, however the effect of this small difference in the temperature should be minimal.

In this evaluation for Davis-Besse, chamfering is not applicable. However, the effect of chamfering of J-groove weld on IDTB weld will be minimal since J-Groove weld chamfering range is away from the triple point. In addition, comparing with transient stresses that determine the ΔK_I, the sustained residual stresses are usually not a major contributor to fatigue crack growth since they do not contribute to ΔK_I, but only to the ratio of the minimum to the maximum stress intensity factor. Therefore, the residual stresses used in Reference (Ref. 16) are considered a reasonable approximation for this flaw evaluation.

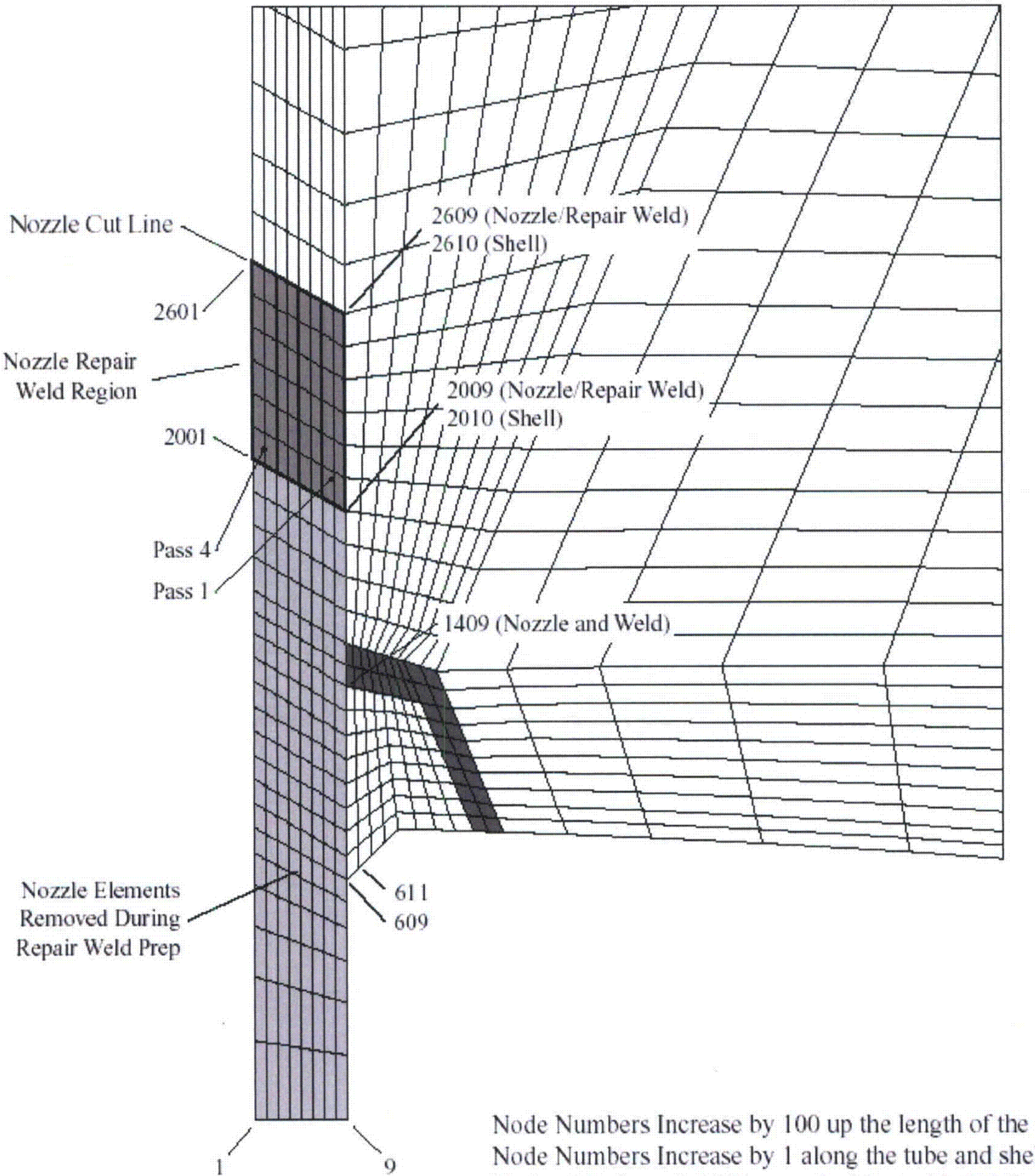

Node Numbers Increase by 100 up the length of the tube and shell
Node Numbers Increase by 1 along the tube and shell radius
Nodes 609 through 1409 are coincident with 610 through 1410

Figure 4-1: FEA Model for Center CRDM Nozzle with Weld Repair

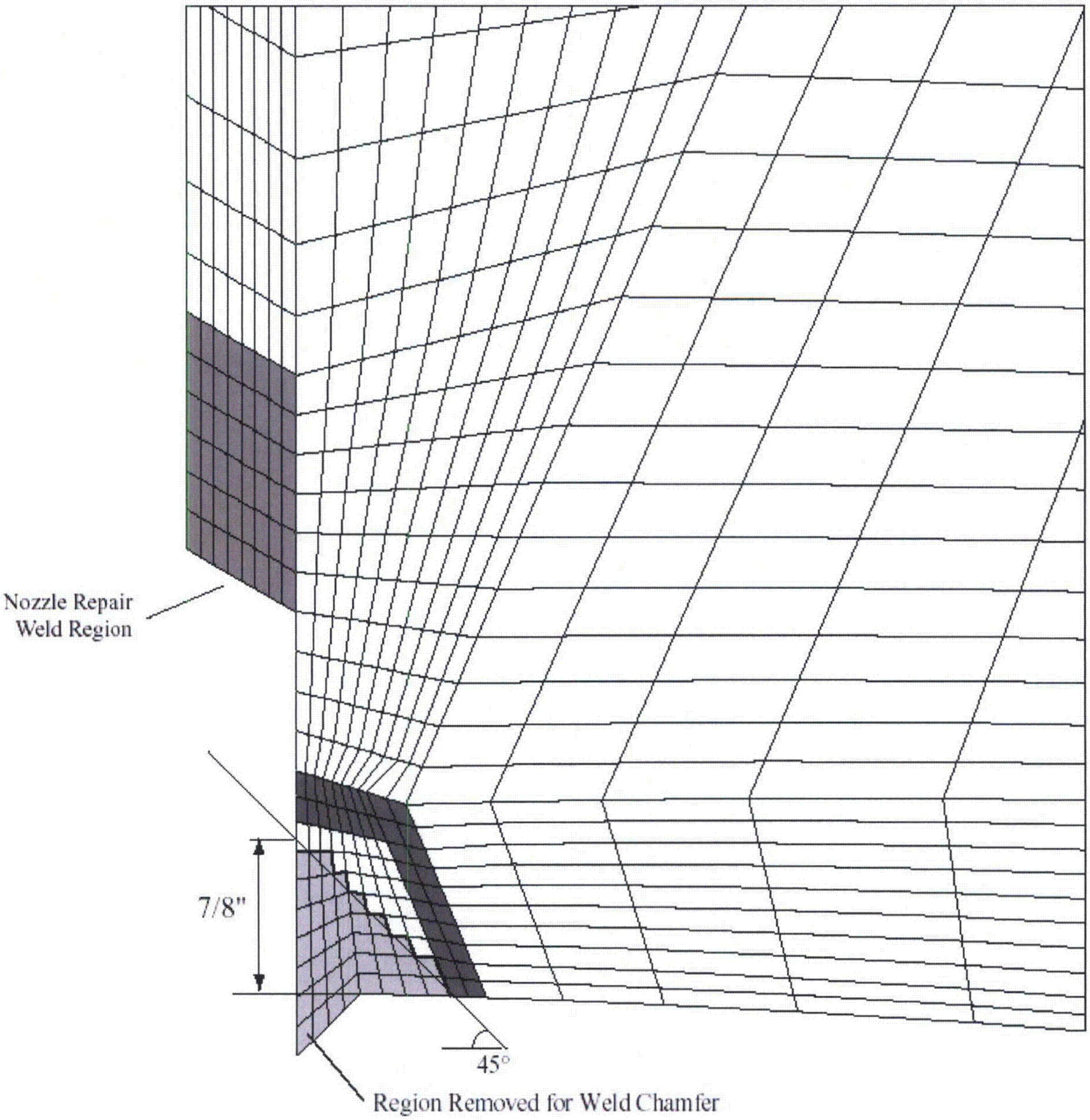

Figure 4-2: FEA Model for Center CRDM Nozzle after Weld Repair and Chamfer*

*Chamfering not applicable for this analysis

Table 4-3: Residual Stresses in Repair Weld after Chamfering* J-Weld

Residual Stresses in Repair Weld after Chamfering J-Weld

Penetration angle = 0 degrees
Nozzle yield strength = [ ]

Time: 16001

Path Along Interface Between Repair Weld and Remaining Nozzle
(Corresponds to Path 1)

Location	Node	Radial Stress (psi)	Hoop Stress (psi)	Axial Stress (psi)	Coordinates X (in.)	Coordinates Z (in.)
Triple Point	2609					
	2608					
	2607					
	2606					
	2605					
	2604					
	2603					
	2602					
Inside Surface	2601					

*Chamfering not applicable for this analysis

Table 4-4: Residual Stresses in Repair weld after Chamfering* J-weld (Cont'd)

Residual Stresses in Repair Weld after Chamfering J-Weld

Penetration angle = 0 degrees
Nozzle yield strength = [ ]

Time: 16001

Path Along Interface Between Repair Weld and Reactor Vessel Head
(Corresponds to Path 2)

Stresses in Weld

Location	Node	Radial Stress (psi)	Hoop Stress (psi)	Axial Stress (psi)	Coordinates X (in.)	Coordinates Z (in.)	Relative Position (in.)
Triple Point	2609						
	2509						
	2409						
	2309						
	2209						
	2109						
Lower End	2009						

Stresses in Head

Location	Node	Radial Stress (psi)	Hoop Stress (psi)	Axial Stress (psi)	Coordinates X (in.)	Coordinates Z (in.)	Relative Position (in.)
Triple Point	2610						
	2510						
	2410						
	2310						
	2210						
	2110						
Lower End	2010						

*Chamfering not applicable for this analysis

4.3 Fracture Toughness

4.3.1 Low Alloy Steel RV Head Material

Fracture toughness curves for SA-533 Grade B Class 1 material are illustrated in Figure A-4200-1 of Reference (Ref. 3). At an operating temperature of about [ ] °F, the K_{Ia} and K_{Ic} fracture toughness values for this material (using an assumed RT_{NDT} of 60°F) are above 200 ksi√in. An upper bound value of 200 ksi√in will be conservatively used for the present flaw evaluations.

4.3.2 Alloy 600 and Alloy 690 Materials

In Table 7 of Reference (Ref.17), Mills provides fracture toughness data for unirradiated Alloy 600 material at 24 °C (75 °F) and 427 °C (800 °F) in the form of crack initiation values for the J-integral, J_c. Using linear interpolation and the LEFM plane strain relationship between J_c and fracture toughness, K_{Jc},

$$K_{Jc} = \sqrt{\frac{J_c E}{1-\nu^2}},$$

the fracture toughness at an operating temperature of [ ]°F is derived as follows:

Note: $\nu = 0.3$
1 kN/m = 1 kN/m ÷ 4.448 N/lb × 0.0254 m/in = 0.00571 kip/in

Temp. (F)	Mills (Ref.17) J_c (kN/m)	J_c (kip/in)	Code (Ref.18) E (ksi)	K_{Jc} (ksi√in)
75	382	2.18	31000	273
[ ]	[ ]	[ ]	[ ]	[ ]
800	575	3.28	27600	316

Since brittle fracture is not a credible failure mechanism for ductile materials like Alloy 600 or Alloy 690, these fracture toughness measures, provided for information only, are not considered in the present flaw evaluations. However, it should be noted that the fracture toughness measures of these ductile materials is significantly greater than the fracture toughness measure of the low alloy RV head material reported in Section 4.3.1. The failure mechanism for the ductile Alloy 600 and 690 materials is limit load.

5.0 CALCULATIONS

The evaluation of the postulated external circumferential flaw for propagation along Path 1 is contained in Tables 5-1 and 5-2. The fatigue crack growth analysis is provided in Table 5-1 and a limit load analysis is presented in Table 5-2.

The evaluation of an external axial flaw for fatigue crack growth along Path 1 is contained in Table 5-3.

A continuous surface flaw along the cylindrical interface between the repair weld and the reactor vessel head is analyzed for fatigue crack growth along Path 2 in Table 5-4.

The flaw evaluations utilize the upset set condition stresses shown in Tables 4-1 and 4-2, which are obtained from heatup/cooldown transient stresses by multiplying the stresses by 1.05 [(psig /   psig)], the ratio of maximum upset condition stresses to heatup/cooldown transient stresses. The stresses used for fatigue crack growth are resulting from the sum of the residual stresses and the transient stresses. This is a conservative approximation of the actual state of stress since the elastic transient stresses are added directly to the elastic-plastic residual stresses, with no attenuation for additional plastic strain. It is therefore appropriate to use the yield strengths from the repair weld residual stress analysis when applying the Irwin plastic zone correction for crack length.

As required by Article IWB-3612 of Reference 3, a safety factor of $\sqrt{10}$ is used to evaluate applied stress intensity factors for normal and upset conditions, considering the lower K_{Ia} fracture toughness for crack arrest. Article IWB-3612 also specifies that a safety factor of $\sqrt{2}$ must be used for emergency and faulted conditions, along with the higher K_{Ic} fracture toughness for crack initiation. Since the required safety margin for the emergency condition rod withdrawal accident is less than that for normal and upset conditions by a factor of $\sqrt{10} / \sqrt{2} = 2.24$ and emergency condition stresses are less than the maximum normal and upset condition stresses (Appendix F, Reference 14), the flaw evaluations performed for normal and upset conditions serve as a bounding analysis for the emergency condition rod withdrawal accident.

Table 5-1: Evaluation of Continuous External Circumferential Flaw for Fatigue Crack Growth along Path 1

INPUT DATA

Geometry:	Outside diameter,	Do =		in.
	Inside diameter,	Di =		in.
	Thickness,	t =		in.
		Ri/t =		
Flaw Size:	Flaw depth,	a =		in.
		a/t =		
Environment:	Temperature,	T =		°F

Table 5-1: Evaluation of Continuous External Circumferential Flaw for Fatigue Crack Growth along Path 1 (Cont'd)

Variation of F Function between Continuous External and Continuous Internal Circumferential Flaws Using Solutions by V. Kumar et al.

Source: EPRI NP-1931 Topical Report, Section 4.3 for an internal circumferential crack under remote tension (Ref. 6).

The applied KI equation is given by the expression:

$$KI = \sigma\sqrt{(\pi a)}F(a/b, Ri/Ro)$$

where

$$\sigma = P/(\pi(Ro^2 - Ri^2))$$

and F is a function of a/b and b/Ri,

where $a/b = 0.177$
$b/Ri = 0.383$

By extrapolation from Table 4-5 of EPRI-1931, the internal F-factor is estimated to be:

$$F_{internal} = 1.12$$

Source: GE Report SRD-82-048, Prepared for EPRI Contract RP-1237-1, Fifth & Sixth Semi-Annual Report, Section 3.5 for an external circumferential under remote tension (Ref. 7).

For the external circumferential crack, the expressions for KI and σ are as defined above for the internal circumferential crack,

where $a/b = 0.177$
$Ri/Ro = 0.723$

From Figure 3-11 of SRD-82-048, the external F-factor is estimated to be:

$$F_{external} = 1.25$$

Multiplying Factor:

To estimate the stress intensity factor for an external circumferential crack from the solution for an internal circumferential crack under remote tension, the appropriate multiplying factor is:

$$F_{external} / F_{internal} = 1.25 / 1.12 \approx 1.12$$

This value seems reasonable since from Figure 3-9 of EPRI NP-3607 (Ref. 8), the multiplying factor for circumferential flaws with an a/t ratio of 0.2 is estimated to be:

$$F_{external} / F_{internal} \approx 1.10$$

Table 5-1: Evaluation of Continuous External Circumferential Flaw for Fatigue Crack Growth along Path 1 (Cont'd)

STRESS INTENSITY FACTOR FOR CIRCUMFERENTIAL FLAW

Basis: Buchalet and Bamford solution for continuous circumferential flaws on the inside surface of cylinders (Ref. 5)

$$KI = \sqrt{(\pi a)}\ [\, A_0 F_1 + (2a/\pi) A_1 F_2 + (a^2/2) A_2 F_3 + (4a^3)/(3\pi) A_3 F_4 \,]$$

where,

$$F1 = 1.1259 + 0.2344(a/t) + 2.2018(a/t)^2 - 0.2083(a/t)^3$$
$$F2 = 1.0732 + 0.2677(a/t) + 0.6661(a/t)^2 + 0.6354(a/t)^3$$
$$F3 = 1.0528 + 0.1065(a/t) + 0.4429(a/t)^2 + 0.6042(a/t)^3$$
$$F4 = 1.0387 - 0.0939(a/t) + 0.6018(a/t)^2 + 0.3750(a/t)^3$$

and the through-wall stress distribution is described by the third order polynomial,

$$S(x) = A_0 + A_1x + A_2x^2 + A_3x^3.$$

Applicablility: $Ri/t = 10$
$a/t \leq 0.8$

Axial Stresses:

Wall Position x	Residual Stress in Weld	Normal/Upset Cond. Stresses		Total Stresses at Operation	
		Cooldown	Shutdown	Cooldown	Shutdown
(in.)	(ksi)	(ksi)	(ksi)	(ksi)	(ksi)

Stress Coefficients:

Stress Coeff.	Normal/Upset Loading Conditions	
	NU1	NU2
	(ksi)	(ksi)
A_0		
A_1		
A_2		
A_3		

Table 5-1: Evaluation of Continuous External Circumferential Flaw for Fatigue Crack Growth along Path 1 (Cont'd)

CRACK GROWTH FOR CIRCUMFERENTIAL FLAW (IN-AIR) - AUSTENITIC MATERIAL

Basis: $\Delta a = \Delta N \; C_o(\Delta KI)^n$ $\Delta N =$ 6 fatigue cycles / year Sy = [ ] ksi

Operating Time (yr.)	Cycle	a (in.)	NU1 KI(a)max (ksi√in)	NU2 KI(a)min (ksi√in)	ΔKI (ksi√in)	R	S	C_o	Δa (in.)	r_y	a_e	NU1 KI(a_e)max (ksi√in)
0	0											
1	6											
2	12											
3	18											
4	24											
5	30											
6	36											
7	42											
8	48											
9	54											
10	60											
11	66											
12	72											
13	78											
14	84											
15	90											
16	96											
17	102											
18	108											
19	114											
20	120											
21	126											
22	132											
23	138											
24	144											
25	150											

Table 5-2: Limit Load Analysis for a Continuous External Circumferential Flaw

LIMIT LOAD

Basis: GE Report SRD-82-048, Combined Fifth and Sixth Semi-Annual Report by V. Kumar et al, Section 3.5 (Ref. 7).

For remote tension loading,

$$Po = 2/\sqrt{3}\, \sigma_o\, \pi\, (Rc^2 - Ri^2)$$

where

Rc = Ro - a

and

σ_o = 27600 psi (conservatively using code minimum yield strength)
Ro = [in.
a = in.
Rc = in.
Ri =] in.

Then

Po = [ ] lbs

From Reference [19], the applied loads on a typical B&W design CRDM tube are:

a) Normal/Upset conditions, P = [lbs
b) Emergency/Faulted conditions, P =] lbs

The limit load margins are greater than those required by Article IWB-3642 of Section XI (Ref. 3), as shown below.

a) Normal/Upset conditions, Po/P = 10.44 > 3.0
b) Emergency/Faulted conditions, Po/P = 7.38 > 1.5

Table 5-3: Evaluation of External Axial Flaw for Fatigue Crack Growth along Path 1

INPUT DATA

Geometry:	Outside diameter,	Do =	[	in.
	Inside diameter,	Di =		in.
	Thickness,	t =		in.
		Ri/t =		
Flaw Size:	Flaw depth,	a =		in.
	Flaw length,	2c=		in.
		a/t =		
Environment:	Temperature,	T =	]	°F

Table 5-3: Evaluation of External Axial Flaw for Fatigue Crack Growth along Path 1 (Cont'd)

STRESS INTENSITY FACTOR FOR AXIAL FLAW

Basis: Raju & Newman, "Stress Intensity Factors for Internal & External Surface Cracks in Cylindrical Vessels (Ref. 9)

$$KI = \sqrt{(\pi/Q)} * [G_0 A_0 a^{0.5} + G_1 A_1 a^{1.5} + G_2 A_2 a^{2.5} + G_3 A_3 a^{3.5}]$$

where, from Table 4 of Reference 9, for an external surface crack with t/R = 0.25, a/t = 0.2, a/c = 1.0, the influence coefficients are as follows:

Location:	Deepest Point ($2\phi/\pi = 1$)	Surface ($2\phi/\pi = 0$)
Go =	1.030	1.163
G_1 =	0.720	0.204
G_2 =	0.591	0.077
G_3 =	0.513	0.040

and **Q =** 2.464 $= (1 + 1.464\,(a/c)^{1.65})$

and the through-wall stress distribution is described by the third order polynomial,

$$S(x) = A_0 + A_1x + A_2x^2 + A_3x^3.$$

Hoop Stresses:

Wall Position x	Residual Stress in Weld	Normal/Upset Cond. Stresses		Total Stresses at Operation	
		Cooldown	Shutdown	Cooldown	Shutdown
(in.)	(ksi)	(ksi)	(ksi)	(ksi)	(ksi)

Stress Coefficients:

Stress Coeff.	Normal/Upset Loading Conditions	
	NU1	NU2
	(ksi)	(ksi)
A_0		
A_1		
A_2		
A_3		

Table 5-3: Evaluation of External Axial Flaw for Fatigue Crack Growth along Path 1 (Cont'd)

RADIAL CRACK GROWTH FOR AXIAL FLAW (IN-AIR) - AUSTENITIC MATERIAL

Basis: $\Delta a = \Delta N\ C_o(\Delta KI)^n$ $\Delta N =$ 6 fatigue cycles / year Sy = [ ] ksi

Operating Time (yr.)	Cycle	a (in.)	NU1 KI(a)max (ksi√in)	NU2 KI(a)min (ksi√in)	ΔKI (ksi√in)	R	S	C_o	Δa (in.)	r_y	a_e	NU1 KI(a_e)max (ksi√in)
0	0											
1	6											
2	12											
3	18											
4	24											
5	30											
6	36											
7	42											
8	48											
9	54											
10	60											
11	66											
12	72											
13	78											
14	84											
15	90											
16	96											
17	102											
18	108											
19	114											
20	120											
21	126											
22	132											
23	138											
24	144											
25	150											

Table 5-3: Evaluation of External Axial Flaw for Fatigue Crack Growth along Path 1 (Cont'd)

AXIAL CRACK GROWTH FOR AXIAL FLAW (IN-AIR) - AUSTENITIC MATERIAL

Basis: $\Delta a = \Delta N * C_o(\Delta KI)^n$ $\Delta N =$ 6 fatigue cycles / year Sy = [ ] ksi

Operating Time (yr.)	Cycle	a (in.)	NU1 KI(a)max (ksi√in)	NU2 KI(a)min (ksi√in)	ΔKI (ksi√in)	R	S	C_o	Δa (in.)	r_y	a_e	NU1 KI(a_e)max (ksi√in)
0	0											
1	6											
2	12											
3	18											
4	24											
5	30											
6	36											
7	42											
8	48											
9	54											
10	60											
11	66											
12	72											
13	78											
14	84											
15	90											
16	96											
17	102											
18	108											
19	114											
20	120											
21	126											
22	132											
23	138											
24	144											
25	150											

Table 5-4: Evaluation of a Continuous Cylindrical Surface Crack for Fatigue Crack Growth along Path 2

INPUT DATA

Geometry:	Plate thickness,	t =		in.
Flaw Size:	Flaw depth,	a =		in.
		a/t =		
Environment:	Temperature,	T =		°F

Table 5-4: Evaluation of a Continuous Cylindrical Surface Crack for Fatigue Crack Growth along Path 2 (Cont'd)

STRESS INTENSITY FACTOR FOR CYLINDRICAL FLAW IN WELD

Basis: Analysis of Flaws, 1995 ASME Code, Section XI, Appendix A (Ref. 3)

$$KI = [\, A_0\, G_0 + A_1\, G_1 + A_2\, G_2 + A_3\, G_3 \,]\ \sqrt{(\pi a/Q)}$$

where $Q = 1 + 4.593\ (a/l)^{1.65} - q_y$

and $q_y = [\ (A_0\, G_0 + A_1\, G_1 + A_2\, G_2 + A_3\, G_3) / \sigma_{ys}\ ]^2 / 6$

For $a/l =$ 0.0 (continuous flaw)
$a/t <=$ 0.1

$G_o =$ 1.195
$G_1 =$ 0.773
$G_2 =$ 0.600
$G_3 =$ 0.501

Stresses are described by a third order polynomial fit over the flaw depth,

$$S(x) = A_0 + A_1(x/a) + A_2(x/a)^2 + A_3(x/a)^3$$

Radial Stresses in Weld:

Wall Position x	Residual Stress in Weld	Normal/Upset Cond. Stresses		Total Stresses at Operation	
		Cooldown	Shutdown	Cooldown	Shutdown
(in.)	(ksi)	(ksi)	(ksi)	(ksi)	(ksi)

Stress Coefficients: (a = 0.100 in.)

Stress Coeff.	Normal/Upset Loading Conditions	
	NU1	NU2
	(ksi)	(ksi)
A_0		
A_1		
A_2		
A_3		

Table 5-4: Evaluation of a Continuous Cylindrical Surface Crack for Fatigue Crack Growth along Path 2 (Cont'd)

CRACK GROWTH FOR CYLINDRICAL FLAW (IN-AIR) - AUSTENITIC MATERIAL

Basis: $\Delta a = \Delta N\ C_o(\Delta KI)^n$ $\Delta N =$ 6 cycles/year Sy = [ ] ksi

Operating Time (yr.)	Cycle	a (in.)	Q	NU1 KI(a)max (ksi√in)	NU2 KI(a)min (ksi√in)	ΔKI (ksi√in)	R	S	C_o	Δa (in.)	q_y	$Q(a_e)$	$KI(a_e)max$ (ksi√in)
0	0												
1	6												
2	12												
3	18												
4	24												
5	30												
6	36												
7	42												
8	48												
9	54												
10	60												
11	66												
12	72												
13	78												
14	84												
15	90												
16	96												
17	102												
18	108												
19	114												
20	120												
21	126												
22	132												
23	138												
24	144												
25	150												

Table 5-4: Evaluation of a Continuous Cylindrical Surface Crack for Fatigue Crack Growth along Path 2 (Cont'd)

STRESS INTENSITY FACTOR FOR CYLINDRICAL FLAW IN HEAD

Basis: Analysis of Flaws, 1995 ASME Code, Section XI, Appendix A (Ref. 3)

$$KI = [\, A_0 G_0 + A_1 G_1 + A_2 G_2 + A_3 G_3 \,] \sqrt{(\pi a/Q)}$$

where $Q = 1 + 4.593\,(a/l)^{1.65} - q_y$

and $q_y = [\,(A_0 G_0 + A_1 G_1 + A_2 G_2 + A_3 G_3) / \sigma_{ys}\,]^2 / 6$

For $a/l =$ 0.0 (continuous flaw)
$a/t <=$ 0.1

$G_o =$ 1.1945
$G_1 =$ 0.7732
$G_2 =$ 0.5996
$G_3 =$ 0.5012

Stresses are described by a third order polynomial fit over the flaw depth,

$$S(x) = A_0 + A_1(x/a) + A_2(x/a)^2 + A_3(x/a)^3$$

Radial Stresses in Weld:

Wall Position x	Residual Stress in Weld	Normal/Upset Cond. Stresses		Total Stresses at Operation	
		Cooldown	Shutdown	Cooldown	Shutdown
(in.)	(ksi)	(ksi)	(ksi)	(ksi)	(ksi)

Stress Coefficients: (a = 0.100 in.)

Stress Coeff.	Normal/Upset Loading Conditions	
	NU1	NU2
	(ksi)	(ksi)
A_0		
A_1		
A_2		
A_3		

Table 5-4: Evaluation of a Continuous Cylindrical Surface Crack for Fatigue Crack Growth along Path 2 (Cont'd)

CRACK GROWTH FOR CYLINDRICAL FLAW (IN-AIR) - FERRITIC MATERIAL

Basis: $\Delta a = \Delta N\ C_o(\Delta KI)^n$ $\Delta N =$ 6 cycles/year Sy = [ ] ksi

Operating Time (yr.)	Cycle	a (in.)	Q	NU1 KI(a)max (ksi√in)	NU2 KI(a)min (ksi√in)	ΔKI (ksi√in)	R	S	C_o	Δa (in.)	q_y	$Q(a_e)$	$KI(a_e)max$ (ksi√in)
0	0												
1	6												
2	12												
3	18												
4	24												
5	30												
6	36												
7	42												
8	48												
9	54												
10	60												
11	66												
12	72												
13	78												
14	84												
15	90												
16	96												
17	102												
18	108												
19	114												
20	120												
21	126												
22	132												
23	138												
24	144												
25	150												

6.0 RESULTS

The flaw evaluation results for 25 years of fatigue crack growth are as follows.

6.1 Propagation of a Continuous External Circumferential Flaw along Path 1

a) Fatigue crack growth analysis:

Initial flaw size,	$a_i = 0.100$ in.
Final flaw size,	$a_f <$ [ ] in.
Stress intensity factor at final flaw size,	$K_I (a_{ef}) <$ 0 ksi√in
Fracture toughness	$K_{Ia} =$ 200 ksi√in
Fracture toughness margin,	$K_{Ia} / K_I >$ √10

b) Limit load analysis:

Limit load,		$P_O =$	[ ] lbs
Applied loads:	normal/upset,	$P =$	[ ] lbs
	emergency/faulted,	$P =$	[ ] lbs
Limit load margins:	normal/upset,	$P_O / P =$	10.44 > 3.0
	emergency/faulted,	$P_O / P =$	7.38 > 1.5

6.2 Fatigue Crack Growth of a Semi-Circular External Axial Flaw along Path 1

Initial flaw size, $a_i = 0.100$ in.

Radial Growth

Final flaw size,	$a_f <$ [ ] in.
Stress intensity factor at final flaw size,	$K_I (a_{ef}) =$ 29.52 ksi√in
Fracture toughness	$K_{Ia} =$ 200 ksi√in
Fracture toughness margin,	$K_{Ia} / K_I =$ 6.78 > √10

Axial Growth

Final flaw size,	$a_f <$ [ ] in.
Stress intensity factor at final flaw size,	$K_I (a_{ef}) =$ 34.57 ksi√in
Fracture toughness	$K_{Ia} =$ 200 ksi√in
Fracture toughness margin,	$K_{Ia} / K_I =$ 5.79 > √10

6.3 Fatigue Crack Growth of a Continuous Cylindrical Flaw along Path 2

Initial flaw size,	$a_i = 0.100$ in.
Final flaw size,	$a_f <$ [ ] in.
Stress intensity factor at final flaw size,	$K_I (a_{ef}) =$ 51.61 ksi√in
Fracture toughness	$K_{Ia} =$ 200 ksi√in
Fracture toughness margin,	$K_{Ia} / K_I =$ 3.88 > √10

The results of the analysis demonstrate that the 0.10 inch weld anomaly is acceptable for a 25 year evaluation life of the CRDM ID temper bead weld repair. However, note that the design life the RVCH as per the design specification (Ref. 2) is 4 years. Significant fracture toughness margins have been demonstrated for both the flaw propagation paths considered in the analysis. The minimum fracture toughness margins for flaw propagation Paths 1 and 2 have been shown to be 5.79 and 3.88, respectively, as compared to the required margins of $\sqrt{10}$ for normal/upset conditions and $\sqrt{2}$ for emergency/faulted conditions per Section XI, IWB-3612 (Ref. 3). Fatigue crack growth is minimal. The maximum final flaw size is [ ] inch (considering both flaw propagation paths). A limit load analysis was also performed considering the ductile Alloy 600 and Alloy 690 materials along flaw propagation Path 1. The analysis showed limit load margins of 10.44 for normal/upset conditions and 7.38 for emergency/faulted conditions, as compared to the required margins of 3.0 and 1.5, respectively, per Section XI, IWB-3642 (Ref. 3).

7.0 REFERENCES

1. AREVA NP Inc Drawing 02-9134305E-002, “Davis Besse CRDM Nozzle ID Temper Bead Weld Repair”.
2. AREVA NP Inc Document 08-9134304-000, “Davis Besse RVCH CRDM Penetration Modification”.
3. ASME Boiler and Pressure Vessel Code, Section XI, Rules for Inservice Inspection of Nuclear Power Plant Components, 1995 Edition with 1996 Addendum.
4. ASME Section II, Part C, “Specification for Welding Rods, Electrodes, and Filler Metals,” 1999 Addenda.
5. C.B. Buchalet and W.H. Bamford, “Stress Intensity Factor Solutions for Continuous Surface Flaws in Reactor Pressure Vessels,” Mechanics of Crack Growth, ASTM STP 590, American Society for Testing and Materials, 1976, pp. 385-402.
6. EPRI Topical Report, EPRI NP-1931, “An Engineering Approach for Elastic-Plastic Fracture Analysis,” Research Project 1237-1, prepared by V. Kumar et al of General Electric Company, July 1981.
7. General Electric Report, SRD-82-048, “Estimation Technique for the Prediction of Elastic-Plastic Fracture of Structural Components of Nuclear Systems,” by V. Kumar et al, Contract RP1237-1, Combined Fifth and Sixth Semi-Annual Report, March 1982.
8. EPRI Topical Report, EPRI NP-3607, “Advances in Elastic-Plastic Fracture Analysis,” Research Project 1237-1, prepared by V. Kumar et al of General Electric Company, August 1984.
9. I.S. Raju and J.C. Newman Jr., “Stress Intensity Factors for Internal and External Surface Cracks in Cylindrical Vessels,” Transactions of the ASME, Journal of Pressure Vessel Technology, pp. 293-298, Vol. 104, November 1982.
10. T.L. Anderson, Fracture Mechanics: Fundamentals and Applications, CRC Press, 1991.
11. AREVA NP Document No.38-1288355-00, “Flaw Acceptance Criteria.”
12. BAW-10046A, Rev. 2, “Methods of Compliance with Fracture Toughness and Operational Requirements of 10 CFR 50, Appendix G,” B&W Owners Group Materials Committee Topical Report, June 1986.
13. FirstEnergy Letter from Jon G. Hook of Davis-Besse Nuclear Power station dated March 30, 2010 to Fred Snow, AREVA NP Inc, “Design Input for Areva calculation 32-9134666-000, DB-1 CRDM Nozzle Weld Anomaly Flaw evaluation of IDTB Repair and other analysis sensitive to RV CRDM nozzle normal operating temperature” (attached in Appendix B).
14. AREVA NP Document No. 32-5012424-12, "CRDM Temper Bead Bore Weld Analysis," April 2004.
15. AREVA NP Document No. 18-1149327-003, "Functional Specification for Reactor Coolant System for Davis-Besse”.
16. AREVA NP Document No. 32-5021539-02, “ANO-1 CRDM Nozzle IDTB Weld Anomaly Flaw Evaluations”.
17. W.J. Mills, “Fracture Toughness of Two Ni-Fe-Cr Alloys,” Hanford Engineering Development Laboratory Document HEDL-SA-3309, April 1985.
18. ASME Boiler and Pressure Vessel Code, Section III, Rules for Construction of Nuclear Power Plant Components, Division 1 – Appendices, 1989 Edition No Addenda
19. AREVA NP Document No. 32-5012403-00, “OC-3 CRDM Nozzle Circumferential Flaw Evaluations”, April 2001.

APPENDIX A: COMPARISION OF DB-1 AND ANO-1 REACTOR VESSEL CLOSURE HEADS

The table below provides comparison of the critical dimensions that are applicable to the DB-1 and ANO-1 reactor vessel replacement closure heads.

Table A-1: Comparison of Critical Dimensions of DB-1 and ANO-1

Table A-2: Comparison of IDTB Materials of DB-1 and ANO-1

As the tables above indicate, the DB1/Midland Head and ANO-1 are identical in geometry and material composition. It is therefore concluded that the Stress calculations for IDTB weld repair for ANO-1 performed in Doc. # 38-1290261-000 (Reference A11) is applicable for the DB-1/Midland replacement RVCH and that resulting residual stresses for the ANO-1 ID temper bead welds are applicable to DB-1 as well.

Appendix References:

APPENDIX B: REFERENCE LETTER FOR OPERATING TEMPERATURE

ENCLOSURE B

AFFIDAVIT FOR

DB-1 CRDM NOZZLE WELD ANOMALY FLAW EVALUATION OF IDTB REPAIR

AREVA CALCULATION 32-9134666-002

Three Pages Follow

AFFIDAVIT

COMMONWEALTH OF VIRGINIA)
) ss.
CITY OF LYNCHBURG)

1. My name is Gayle F. Elliott. I am Manager, Product Licensing, for AREVA NP Inc. and as such I am authorized to execute this Affidavit.

2. I am familiar with the criteria applied by AREVA NP to determine whether certain AREVA NP information is proprietary. I am familiar with the policies established by AREVA NP to ensure the proper application of these criteria.

3. I am familiar with the AREVA NP information contained in Calculation Summary Sheet (CSS) 32-9134666-002 entitled "DB-1 CRDM Nozzle Weld Anomaly Flaw Evaluation of IDTB Repair," dated April 2010 and referred to herein as "Document." Information contained in this Document has been classified by AREVA NP as proprietary in accordance with the policies established by AREVA NP for the control and protection of proprietary and confidential information.

4. This Document contains information of a proprietary and confidential nature and is of the type customarily held in confidence by AREVA NP and not made available to the public. Based on my experience, I am aware that other companies regard information of the kind contained in this Document as proprietary and confidential.

5. This Document has been made available to the U.S. Nuclear Regulatory Commission in confidence with the request that the information contained in this Document be withheld from public disclosure. The request for withholding of proprietary information is made in accordance with 10 CFR 2.390. The information for which withholding from disclosure is

requested qualifies under 10 CFR 2.390(a)(4) "Trade secrets and commercial or financial information."

6. The following criteria are customarily applied by AREVA NP to determine whether information should be classified as proprietary:

(a) The information reveals details of AREVA NP's research and development plans and programs or their results.

(b) Use of the information by a competitor would permit the competitor to significantly reduce its expenditures, in time or resources, to design, produce, or market a similar product or service.

(c) The information includes test data or analytical techniques concerning a process, methodology, or component, the application of which results in a competitive advantage for AREVA NP.

(d) The information reveals certain distinguishing aspects of a process, methodology, or component, the exclusive use of which provides a competitive advantage for AREVA NP in product optimization or marketability.

(e) The information is vital to a competitive advantage held by AREVA NP, would be helpful to competitors to AREVA NP, and would likely cause substantial harm to the competitive position of AREVA NP.

The information in the Document is considered proprietary for the reasons set forth in paragraphs 6(b) and 6(c) above.

7. In accordance with AREVA NP's policies governing the protection and control of information, proprietary information contained in this Document have been made available, on a limited basis, to others outside AREVA NP only as required and under suitable agreement providing for nondisclosure and limited use of the information.

8. AREVA NP policy requires that proprietary information be kept in a secured file or area and distributed on a need-to-know basis.

9. The foregoing statements are true and correct to the best of my knowledge, information, and belief.

SUBSCRIBED before me this 8th

day of April 2010.

Sherry L. McFaden
NOTARY PUBLIC, COMMONWEALTH OF VIRGINIA
MY COMMISSION EXPIRES: 10/31/10
Reg. # 7079129

SHERRY L. McFADEN
Notary Public
Commonwealth of Virginia
7079129
My Commission Expires Oct 31, 2010